

Vol. 7 (2025), no. 1, pp. 49–68

http://doi.org/10.62071/tmjm.v7i1.794

ISSN: 2094-7380 (Print) | 2783-0136 (Online)

MATHEMATICAL MODEL OF DENGUE AND LEPTOSPIROSIS COINFECTION WITH DUAL TRANSMISSION PATHWAYS

Rhea T. Merontos^{1,*}, Randy L. Caga-anan², & Thomas Goetz³

1,2Department of Mathematics and Statistics
MSU-Iligan Institute of Technology, 9200 Iligan City, Philippines
rhea.merontos@g.msuiit.edu.ph, randy.caga-anan@g.msuiit.edu.ph

³Mathematical Institute University of Koblenz, D-56070 Koblenz, Germany goetz@uni-koblenz.de

Received: 3rd May 2025 Revised: 1st July 2025

Abstract

Dengue and leptospirosis are major public health concerns in tropical countries, where environmental conditions favor the spread of both vector-borne and waterborne pathogens. This paper presents a compartmental mathematical model that captures the coinfection dynamics of dengue and leptospirosis, accounting for their indirect transmission routes and potential interactions. The model incorporates both mosquito vectors for dengue and a contaminated water compartment for leptospirosis, allowing for dual transmission pathways through which each disease spreads. The disease-free equilibrium is established, and the basic reproduction number \mathcal{R}_0 is derived using the next-generation matrix approach. Model analysis shows that the disease-free equilibrium is locally asymptotically stable when \mathcal{R}_0 1, and unstable otherwise. Numerical simulations reveal that if the basic reproduction number is greater than one, the infection persists in the population. Sensitivity analysis highlights that transmission rates significantly increase infection risk, while recovery and decay parameters contribute to disease mitigation. These findings emphasize the importance of integrated control strategies targeting both vector and water environments. Future studies may extend this model by incorporating optimal control interventions, seasonal climate effects, or vaccination strategies to better understand and manage coinfection dynamics.

1 Introduction

The Philippines, with its tropical climate and frequent rainfall, provides a conducive environment for the spread of vector-borne and waterborne diseases. Vector-borne diseases are illnesses caused by parasites, viruses, or bacteria that are transmitted by vectors such as mosquitoes, ticks, sandflies, fleas, and lice [24]. Several diseases are classified as vector-borne, with dengue fever being one of the most prevalent. Dengue is caused by the dengue virus and is primarily transmitted by Aedes aegypti and Aedes albopictus mosquitoes. Other well-known vector-borne diseases include malaria, caused by Plasmodium parasites and transmitted by Anopheles

mosquitoes, and Zika virus, which is also spread by Aedes mosquitoes and is associated with neurological complications. Environmental conditions influence vector behavior and survival, contributing to disease transmission dynamics [3]. On the other hand, waterborne diseases are caused by pathogenic microorganisms such as bacteria, viruses, protozoa, and parasites that spread through contaminated water sources [13]. These diseases disproportionately affect populations without access to clean water and adequate sanitation. Infections are typically acquired through the consumption of or contact with contaminated water, or indirectly through surfaces exposed to infectious water [18]. One of the most significant waterborne diseases in tropical and subtropical areas is leptospirosis, caused by the *Leptospira* bacterium [17]. This bacterium, commonly found in the urine of infected animals like rodents, can persist in freshwater for extended periods. Humans usually contract the disease through exposure to contaminated water, especially during floods or when wading in stagnant water [11]. Coinfection with diseases such as dengue and leptospirosis presents a serious public health challenge due to overlapping symptoms such as fever, muscle pain, and headache. These similarities complicate diagnosis and treatment, increasing the risk of misdiagnosis and placing additional pressure on healthcare systems [21].

Mathematical modeling is a powerful tool for understanding the transmission dynamics of infectious diseases and evaluating intervention strategies. Classical models such as the Ross-Macdonald model have provided foundational insights into vector-borne disease transmission [19, 15], while models for waterborne diseases often include environmental compartments to account for indirect transmission. Although many studies have investigated dengue and leptospirosis individually, few have explored their combined dynamics, especially in the context of coinfection. This study proposes a new mathematical model that captures the coinfection dynamics of dengue and leptospirosis by incorporating their distinct transmission pathways: vector-borne for dengue and waterborne for leptospirosis. In contrast to earlier studies like that of Alemneh et al. [1], which used general assumptions about direct transmission and simple SIR models, this study presents a more realistic model based on how the diseases actually spread. For dengue, an SIR framework is used to reflect that people gain immunity after recovery. For leptospirosis, an SIWR [20] structure is applied to include the role of contaminated water in spreading the disease. By explicitly modeling both mosquito dynamics and environmental contamination, the framework provides a realistic portrayal of how these diseases spread in tropical regions, especially under conditions of flooding and poor sanitation. It captures the potential interaction between the two pathways, which are typically examined separately in existing studies.

2 Model Formulation

The total human population at time t, denoted by $N_H(t)$, is subdivided into seven compartments denoted by the following variables: $S_H(t)$ represents the number of susceptible individuals, $I_V(t)$ denotes the number of individuals infected with the vector-borne disease, $I_W(t)$ represents the number of individuals infected with the waterborne disease, and $I_{VW}(t)$ accounts for those infected with both diseases. The recovered compartments include $R_V(t)$ for individuals who recovered from the vector-borne disease, $R_W(t)$ for those who recovered from the waterborne disease, and $R_{VW}(t)$ for individuals who recovered from both diseases. The vector population consists of susceptible (S_A) and infected (I_A) compartments, while the water compartment (W) represents the concentration of pathogens from the waterborne infection.

Individuals are assumed to enter the human population through birth and are initially susceptible. The total human population is considered constant, as birth and natural death occur at the same rate, denoted by μ_H . Susceptible humans S_H can become infected in two ways;

through contact with infected vectors or exposure to contaminated water. The vector-borne transmission occurs when a susceptible human is bitten by an infected mosquito, with infection occurring at a rate proportional to the density of infected vectors, modeled by $\beta_V \frac{I_A}{N_H}$. In contrast, waterborne transmission is governed by the environmental concentration of pathogens, such that individuals in S_H move to I_W at a rate $\beta_W W$. Once infected with a single disease, individuals may follow different pathways. Those in the vector-infected class I_V may recover at rate η_V and move to R_V , or may acquire a secondary waterborne infection, transitioning to the coinfected class I_{VW} . Similarly, individuals in the water-infected class I_W may recover at rate η_W and move to R_W , or acquire a secondary vector-borne infection, also entering I_{VW} . Coinfected individuals in I_{VW} recover from both diseases at a combined rate φ and move to the recovery class R_{VW} . All human compartments are subject to natural mortality at rate μ_H , and there is no reinfection from recovery classes, as immunity is assumed.

The mosquito vector population S_A increases through birth rate $\mu_A N_A$, and declines due to infection from biting humans in I_V and I_{VW} , which causes transition to the infected vector class I_A at rate $\rho_A \frac{I_V + I_{VW}}{N_H}$. Infected vectors die at rate μ_A , and do not recover, modeling lifelong infectiousness. For the water component W, the concentration of pathogen in water increases due to bacterial shedding from individuals in I_W and I_{VW} , at rate θ , and declines through natural decay at rate δ . The water compartment W tracks the concentration of bacterial pathogens in the environment. This compartment increases as infected individuals in I_W and I_{VW} shed bacteria into the water at a constant rate θ , representing contributions through urine, feces, or bodily fluids [4]. The pathogen load in the water decreases over time due to natural decay at a constant rate δ . The flow diagram of the model is given in Figure 1.

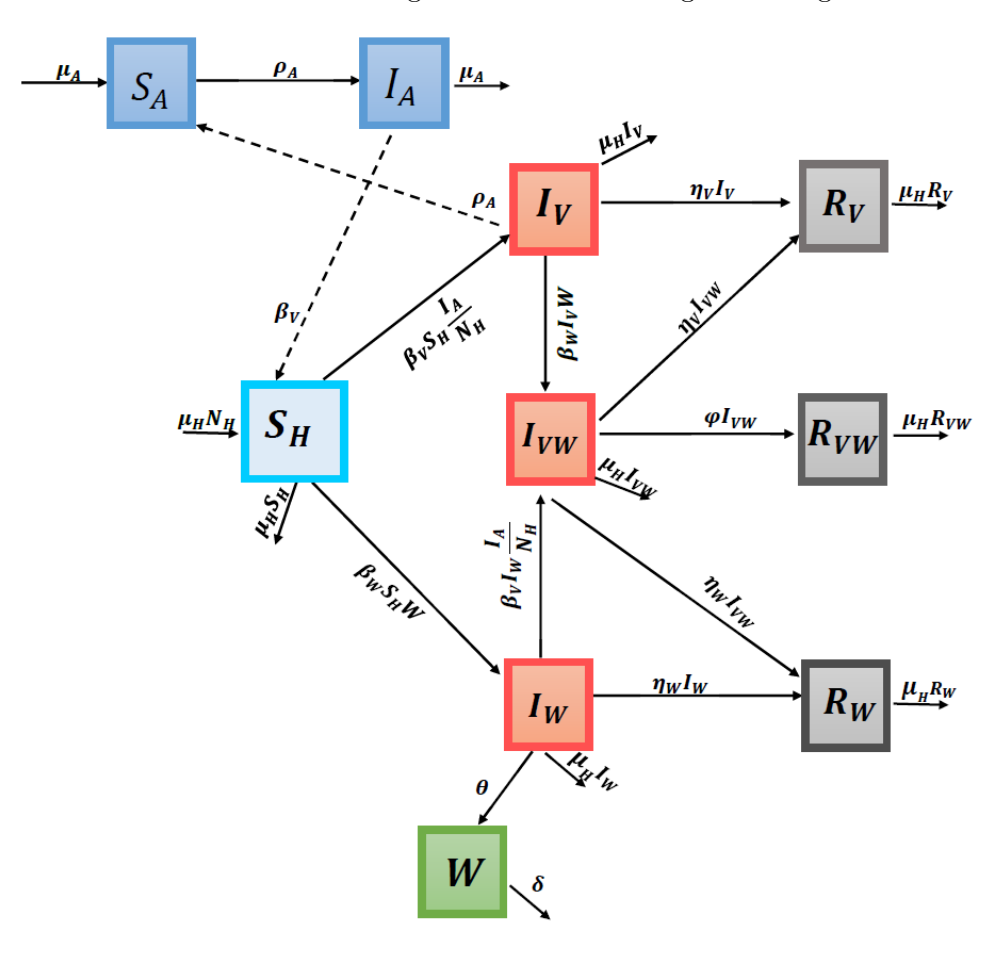


Figure 1: State-flow diagram of the proposed model.



The epidemic model is described by the following system of differential equations:

$$\frac{dS_H}{dt} = \mu_H N_H - \beta_V S_H \frac{I_A}{N_H} - \beta_W S_H W - \mu_H S_H \tag{1}$$

$$\frac{dI_V}{dt} = \beta_V S_H \frac{I_A}{N_H} - \beta_W I_V W - (\eta_V + \mu_H) I_V \tag{2}$$

$$\frac{dI_W}{dt} = \beta_W S_H W - \beta_V I_W \frac{I_A}{N_H} - (\eta_W + \mu_H) I_W \tag{3}$$

$$\frac{dI_{VW}}{dt} = \beta_W I_V W + \beta_V I_W \frac{I_A}{N_H} - (\eta_V + \eta_W + \varphi + \mu_H) I_{VW}$$
 (4)

$$\frac{dR_V}{dt} = \eta_V (I_V + I_{VW}) - \mu_H R_V \tag{5}$$

$$\frac{dR_W}{dt} = \eta_W \left(I_W + I_{VW} \right) - \mu_H R_W \tag{6}$$

$$\frac{dR_{VW}}{dt} = \varphi I_{VW} - \mu_H R_{VW} \tag{7}$$

$$\frac{dS_A}{dt} = \mu_A N_A - \frac{\rho_A \left(I_V + I_{VW} \right)}{N_H} S_A - \mu_A S_A \tag{8}$$

$$\frac{dI_A}{dt} = \frac{\rho_A (I_V + I_{VW})}{N_H} S_A - \mu_A I_A \tag{9}$$

$$\frac{dW}{dt} = \theta(I_W + I_{VW}) - \delta W. \tag{10}$$

This system of equations is epidemiologically and mathematically well-posed on the domain

$$D = \left\{ (S_H, I_V, I_W, I_{VW}, R_V, R_W, R_{VW}, S_A, I_A, W) \in \mathbb{R}^{10}_+ \mid S_H > 0, I_V \ge 0, I_W \ge 0, I_{VW} \ge 0, R_V \ge 0, R_W \ge 0, R_{VW} \ge 0, S_A > 0, I_A \ge 0, W \ge 0 \right\}.$$

The space \mathbb{R}^{10}_+ denotes the positive orthant in \mathbb{R}^{10} .

3 Main Results

3.1 Model Analysis

Theorem 3.1. Assuming that the initial conditions lie in D, the system of equations (1) - (10) has a unique solution that exists and remains nonnegative in D for all time $t \ge 0$.

Proof. The right-hand side of the system of equations (1)–(10) is continuous with continuous partial derivatives in D. Hence, by the Cauchy-Lipschitz theorem, the system admits a unique local solution for initial conditions in D.

We now show that the set D is positively invariant, that is, any solution starting in D remains in D for all $t \geq 0$. This is equivalent to showing that each compartment remains nonnegative over time.

Consider $S_H = 0$. Then,

$$\frac{dS_H}{dt} = \mu_H N_H > 0,$$

which implies that $S_H(t)$ remains nonnegative for all $t \ge 0$. Similarly, if $I_V = I_W = I_{VW} = 0$ and $I_A, W \ge 0$, then

$$\begin{split} \frac{dI_V}{dt} &= \beta_V S_H \frac{I_A}{N_H} \geq 0, \\ \frac{dI_W}{dt} &= \beta_W S_H W \geq 0, \\ \frac{dI_{VW}}{dt} &= \beta_W I_V W + \beta_V I_W \frac{I_A}{N_H} \geq 0. \end{split}$$

Thus, $I_V(t)$, $I_W(t)$, and $I_{VW}(t)$ remain nonnegative for all $t \ge 0$. If $R_V = R_W = R_{VW} = 0$, then

$$\frac{dR_V}{dt} = \eta_V(I_V + I_{VW}) \ge 0,$$

$$\frac{dR_W}{dt} = \eta_W(I_W + I_{VW}) \ge 0,$$

$$\frac{dR_{VW}}{dt} = \varphi I_{VW} \ge 0,$$

so $R_V(t)$, $R_W(t)$, and $R_{VW}(t)$ remain nonnegative for all $t \ge 0$. For the vector and environmental compartments, if $S_A = 0$, then

$$\frac{dS_A}{dt} = \mu_A N_A \ge 0,$$

and if $I_A = 0$, then

$$\frac{dI_A}{dt} = \frac{\rho_A(I_V + I_{VW})}{N_H} S_A \ge 0.$$

Also, if W = 0, then

$$\frac{dW}{dt} = \theta(I_W + I_{VW}) \ge 0.$$

Hence, $S_A(t)$, $I_A(t)$, and W(t) also remain nonnegative for all $t \ge 0$. Hence, all state variables remain in the nonnegative orthant for all $t \ge 0$, and the set D is positively invariant.

Now, to show boundedness, define the total human and vector populations by

$$N_H(t) = S_H(t) + I_V(t) + I_W(t) + I_{VW}(t) + R_V(t) + R_W(t) + R_{VW}(t),$$

$$N_A(t) = S_A(t) + I_A(t).$$

Adding equations (1)–(7) and using the fact that the birth and death rates are equal,

$$\frac{dN_H}{dt} = \mu_H N_H - \mu_H N_H = 0 \quad \Rightarrow \quad N_H(t) = N_H(0) \quad \text{for all } t \ge 0.$$

Similarly, adding equations (8)–(9),

$$\frac{dN_A}{dt} = \mu_A N_A - \mu_A N_A = 0 \quad \Rightarrow \quad N_A(t) = N_A(0) \quad \text{for all } t \ge 0.$$

Thus, the human and vector populations remain constant and bounded. Since all compartments are nonnegative and their sums are bounded above by $N_H(0)$ and $N_A(0)$, each state variable is uniformly bounded on $[0, \infty)$. Therefore, the local solution remains in D for all $t \ge 0$.



Definition 3.2. [2]A steady state solution is a solution to the system that is constant for any time t. That is, a solution $(S_H(t), I_V(t), I_W(t), I_{VW}(t), R_V(t), R_W(t), R_{VW}(t), S_A(t), I_A(t), W(t))$ such that

$$\left(\frac{dS_H}{dt},\frac{dI_V}{dt},\frac{dI_W}{dt},\frac{dI_{VW}}{dt},\frac{dR_V}{dt},\frac{dR_W}{dt},\frac{dR_{VW}}{dt},\frac{dS_A}{dt},\frac{dI_A}{dt},\frac{dW}{dt}\right) = \vec{0}.$$

Definition 3.3. [2] A disease-free equilibrium (DFE) is a steady state solution of an epidemic model with all infected variables equal to zero.

Theorem 3.4. The disease free equilibrium (DFE) point of the model in (1) - (10) is given by

$$E_0 = (N_H, 0, 0, 0, 0, 0, 0, N_A, 0, 0).$$

Proof. Let $(S_H, I_V, I_W, I_{VW}, R_V, R_W, R_{VW}, S_A, I_A, W)$ be a DFE point. Then $I_V = I_W = I_{VW} = I_A = W = 0$ and $\left(\frac{dS_H}{dt}, \frac{dI_V}{dt}, \frac{dI_W}{dt}, \frac{dI_V}{dt}, \frac{dR_V}{dt}, \frac{dR_W}{dt}, \frac{dR_{VW}}{dt}, \frac{dS_A}{dt}, \frac{dI_A}{dt}, \frac{dW}{dt}\right) = \vec{0}$. Substituting these values to our system of equations (1) - (10), we have

$$\mu_H N_H - \mu_H S_H = 0$$
$$\mu_A N_A - \mu_A S_A = 0.$$

Since $\mu_A, \mu_H > 0$, we get $S_H = N_H$ and $S_A = N_A$.

3.2 Reproduction Number

The basic reproduction number for a compartmental model is computed by using the next-generation matrix method. This method was initially introduced by Diekmann et al. [6] and P. van den Driessche and Watmough [22]. In the next generation method, \mathcal{R}_0 is defined as the largest eigenvalue or spectral radius of the next generation operator K. The formation of K involves in formulating the infected and non-infected compartments from the model equations.

Definition 3.5. [6] The basic reproduction number, \mathcal{R}_0 is the average number of secondary infectious cases when a single infectious individual is introduced into the whole susceptible population. The disease dies out if the basic reproduction number $\mathcal{R}_0 < 1$, and the disease persists whenever $\mathcal{R}_0 > 1$.

Theorem 3.6. The basic reproduction number for system (1)-(10) is $\mathcal{R}_0 = \max\{\mathcal{R}_1, \mathcal{R}_2\}$ where

$$\mathcal{R}_1 = \sqrt{\frac{\rho_A \beta_V N_A}{\mu_A (\eta_V + \mu_H) N_H}} \text{ and } \mathcal{R}_2 = \sqrt{\frac{\theta \beta_W N_H}{\delta (\eta_W + \mu_H)}}.$$

Proof. Let **X** be a vector of infected classes and **Y** be a vector of the other classes. Hence,

$$\mathbf{X} = egin{bmatrix} I_V \\ I_W \\ I_{VW} \\ I_A \\ W \end{bmatrix}, \mathbf{Y} = egin{bmatrix} S_H \\ R_V \\ R_{WW} \\ S_A \end{bmatrix}.$$

Let $\mathcal{F}(\mathbf{X}, \mathbf{Y})$ be the vector of new infection rates(flows from \mathbf{Y} to \mathbf{X}) and let $\mathcal{V}(\mathbf{X}, \mathbf{Y})$ be the vector of all other rates (not new infections). Then,

$$\mathcal{F}(\mathbf{X}) = \begin{bmatrix} \frac{\beta_{V}S_{H}I_{A}}{N_{H}} \\ \beta_{W}S_{H}W \\ \beta_{W}I_{V}W + \frac{\beta_{V}I_{W}I_{A}}{N_{H}} \\ \frac{\rho_{A}(I_{V}+I_{VW})S_{A}}{N_{H}} \\ \theta(I_{W}+I_{VW}) \end{bmatrix} = \begin{bmatrix} \mathcal{F}_{1} \\ \mathcal{F}_{2} \\ \mathcal{F}_{3} \\ \mathcal{F}_{4} \\ \mathcal{F}_{5} \end{bmatrix}$$

$$\mathcal{V}(\mathbf{X}) = \begin{bmatrix} \beta_{W}I_{V}W + (\eta_{V}+\mu_{H})I_{V} \\ \beta_{V}I_{W}\frac{I_{A}}{N_{H}} + (\eta_{W}+\mu_{H})I_{W} \\ (\eta_{V}+\eta_{W}+\varphi+\mu_{H})I_{VW} \\ \mu_{A}I_{A} \\ \delta W \end{bmatrix} = \begin{bmatrix} \mathcal{V}_{1} \\ \mathcal{V}_{2} \\ \mathcal{V}_{3} \\ \mathcal{V}_{4} \\ \mathcal{V}_{5} \end{bmatrix}.$$

The next generation operator formed is $K = FV^{-1}$ where $F = \left[\frac{\partial \mathcal{F}(E_0)}{\partial \mathbf{X}}\right]$ and $V = \left[\frac{\partial \mathcal{V}(E_0)}{\partial \mathbf{X}}\right]$, where E_0 is the disease-free equilibrium. This becomes

$$F = \begin{bmatrix} 0 & 0 & 0 & \beta_{V} & 0 \\ 0 & 0 & 0 & 0 & \beta_{W} N_{H} \\ 0 & 0 & 0 & 0 & 0 \\ \frac{\rho_{A} N_{A}}{N_{H}} & 0 & \frac{\rho_{A} N_{A}}{N_{H}} & 0 & 0 \\ 0 & \theta & \theta & 0 & 0 \end{bmatrix},$$

$$V = \begin{bmatrix} \eta_{V} + \mu_{H} & 0 & 0 & 0 & 0 \\ 0 & \eta_{W} + \mu_{H} & 0 & 0 & 0 & 0 \\ 0 & 0 & \eta_{V} + \eta_{W} + \varphi + \mu_{H} & 0 & 0 \\ 0 & 0 & 0 & 0 & 0 & \delta \end{bmatrix}.$$

Thus, the next generation matrix is given by

$$\begin{split} & = FV^{-1} \\ & = \begin{bmatrix} 0 & 0 & 0 & \beta_V & 0 \\ 0 & 0 & 0 & 0 & \beta_W N_H \\ 0 & 0 & 0 & 0 & 0 \\ \frac{\rho_A N_A}{N_H} & 0 & \frac{\rho_A N_A}{N_H} & 0 & 0 \\ 0 & \theta & \theta & 0 & 0 \end{bmatrix} \begin{bmatrix} \frac{1}{\eta_V + \mu_H} & 0 & 0 & 0 & 0 \\ 0 & \frac{1}{\eta_W + \mu_H} & 0 & 0 & 0 \\ 0 & 0 & \frac{1}{\eta_V + \eta_W + \varphi + \mu_H} & 0 & 0 \\ 0 & 0 & 0 & 0 & \frac{1}{\mu_A} & 0 \\ 0 & 0 & 0 & 0 & \frac{1}{\delta} \end{bmatrix} \\ & = \begin{bmatrix} 0 & 0 & 0 & \frac{\beta_V}{\mu_A} & 0 \\ 0 & 0 & 0 & \frac{\beta_W N_H}{\delta} \\ 0 & 0 & 0 & 0 & 0 \\ \frac{\rho_A N_A}{N_H (\eta_V + \mu_H)} & 0 & 0 & 0 \\ 0 & \frac{\rho_A N_A}{\eta_V + \eta_W + \varphi + \mu_H} & 0 & 0 \end{bmatrix}. \end{split}$$

Solving for eigenvalues of K, the characteristic matrix $K - \lambda I$ is given by

$$K - \lambda I = \begin{bmatrix} -\lambda & 0 & 0 & \frac{\beta_V}{\mu_A} & 0\\ 0 & -\lambda & 0 & 0 & \frac{\beta_W N_H}{\delta}\\ 0 & 0 & -\lambda & 0 & 0\\ \frac{\rho_A N_A}{N_H (\eta_V + \mu_H)} & 0 & \frac{\rho_A N_A}{N_H (\eta_V + \eta_W + \varphi + \mu_H)} & -\lambda & 0\\ 0 & \frac{\theta}{\eta_W + \mu_H} & \frac{\theta}{\eta_V + \eta_W + \varphi + \mu_H} & 0 & -\lambda \end{bmatrix}$$



and by cofactor expansion, the determinant is computed as

$$\det |K - \lambda I| = 0$$

$$-\lambda \left[\lambda^2 \left(\lambda^2 - \frac{\theta \beta_W N_H}{\delta(\eta_W + \mu_H)} \right) - \frac{\rho_A \beta_V N_A}{\mu_A(\eta_V + \mu_H) N_H} \left(\lambda^2 - \frac{\theta \beta_W N_H}{\delta(\eta_W + \mu_H)} \right) \right] = 0$$

$$-\lambda \left[\left(\lambda^2 - \frac{\rho_A \beta_V N_A}{\mu_A(\eta_V + \mu_H) N_H} \right) \left(\lambda^2 - \frac{\theta \beta_W N_H}{\delta(\eta_W + \mu_H)} \right) \right] = 0.$$

The eigenvalues are

$$\lambda = 0,$$

$$\lambda^2 - \frac{\rho_A \beta_V N_A}{\mu_A (\eta_V + \mu_H) N_H} = 0 \implies \lambda = \pm \sqrt{\frac{\rho_A \beta_V N_A}{\mu_A (\eta_V + \mu_H) N_H}} \quad \text{and}$$

$$\lambda^2 - \frac{\theta \beta_W N_H}{\delta (\eta_W + \mu_H)} = 0 \implies \lambda = \pm \sqrt{\frac{\theta \beta_W N_H}{\delta (\eta_W + \mu_H)}}.$$

Thus, by taking the dominant eigenvalue of matrix K, we have $\mathcal{R}_0 = \max\{\mathcal{R}_1, \mathcal{R}_2\}$ where

$$\mathcal{R}_1 = \sqrt{\frac{\rho_A \beta_V N_A}{\mu_A (\eta_V + \mu_H) N_H}} \text{ and } \mathcal{R}_2 = \sqrt{\frac{\theta \beta_W N_H}{\delta (\eta_W + \mu_H)}}.$$

Here, \mathcal{R}_1 captures the contribution from vector-borne transmission, while \mathcal{R}_2 reflects the effect of waterborne transmission.

3.3 Stability of the disease-free equilibrium point

The stability of the equilibrium point can be performed by calculating the roots of the eigenequation

$$\det(J(E_0) - I_{10}\lambda) = 0$$

where $J(E_0)$ is the Jacobian evaluated at the equilibrium point, and I_{10} is the identity matrix. Since there are ten differential equations, the characteristic polynomial of degree 10. Let the matrix for equations (1) - (10) be given by

where the independent variables are

$$\begin{bmatrix} S_H & I_V & I_W & I_{VW} & R_V & R_W & R_{VW} & S_A & I_A & W \end{bmatrix}^T = \begin{bmatrix} x_1 & x_2 & x_3 & x_4 & x_5 & x_6 & x_7 & x_8 & x_9 & x_{10} \end{bmatrix}^T.$$

The superscript T refers to transpose of the matrix.

Hence,
$$J(x_1, x_2, ..., x_{10}) = \left[\frac{\partial y_i}{\partial x_j}\right]$$
 for $i = 1, ..., 10$. The Jacobian matrix is the 10×10

matrix given by

$$J(x_1, x_2, \dots, x_{10}) = \begin{bmatrix} J_{11} & 0 & 0 & 0 & 0 & 0 & 0 & 0 & J_{19} & J_{1,10} \\ J_{21} & J_{22} & 0 & 0 & 0 & 0 & 0 & 0 & 0 & J_{29} & J_{2,10} \\ J_{31} & 0 & J_{33} & 0 & 0 & 0 & 0 & 0 & J_{39} & J_{3,10} \\ 0 & J_{42} & J_{43} & J_{44} & 0 & 0 & 0 & 0 & J_{49} & J_{4,10} \\ 0 & J_{52} & 0 & J_{54} & J_{55} & 0 & 0 & 0 & 0 & 0 \\ 0 & 0 & J_{63} & J_{64} & 0 & J_{66} & 0 & 0 & 0 & 0 \\ 0 & 0 & 0 & J_{74} & 0 & 0 & J_{77} & 0 & 0 & 0 \\ 0 & J_{82} & 0 & J_{84} & 0 & 0 & 0 & J_{88} & 0 & 0 \\ 0 & J_{92} & 0 & J_{94} & 0 & 0 & 0 & J_{98} & J_{99} & 0 \\ 0 & 0 & J_{10,3} & J_{10,4} & 0 & 0 & 0 & 0 & 0 & J_{10,10} \end{bmatrix}$$

where,

Theorem 3.7. [2, Theorem 2] Let $A \in \mathbb{R}_{n \times n}$. Let \mathbf{u}^* be the equilibrium point of the initial value problem

$$\mathbf{u}'(t) = A\mathbf{u}(t)$$

 $\mathbf{u}(0) = \mathbf{u}_0.$



This equilibrium is:

- (i) locally asymptotically stable if $\forall \lambda \in \sigma(A), Re(\lambda) < 0$;
- (ii) stable if $\forall \lambda \in \sigma(A)$, $Re(\lambda) < 0$ or $Re(\lambda) = 0$ and $\dim(Ker(A \lambda I)) = m$, where m is the multiplicity of λ ;
- (iii) unstable if $\exists \lambda \in \sigma(A), Re(\lambda) > 0$,

where $\sigma(A)$ is the set of eigenvalues of A, $Re(\lambda)$ represents the real part of the eigenvalue λ and $\dim(Ker(A-\lambda I))$ denotes the dimension of the kernel (null space) of the matrix $(A-\lambda I)$, where λ is an eigenvalue of A.

Theorem 3.8. The disease-free equilibrium point $(N_H, 0, 0, 0, 0, 0, 0, N_A, 0, 0)$ is locally asymptotically stable if $\mathcal{R}_0 < 1$ and unstable if $\mathcal{R}_0 > 1$.

Proof. The Jacobian matrix of the system at disease-free equilibrium (DFE) is given by

$$J = \begin{bmatrix} -\mu_H & 0 & 0 & 0 & 0 & 0 & 0 & 0 & 0 & -\beta_V & -\beta_W N_H \\ 0 & -(\eta_V + \mu_H) & 0 & 0 & 0 & 0 & 0 & 0 & 0 & \beta_V & 0 \\ 0 & 0 & -(\eta_W + \mu_H) & 0 & 0 & 0 & 0 & 0 & 0 & 0 & \beta_W N_H \\ 0 & 0 & 0 & -(\eta_V + \eta_W + \varphi + \mu_H) & 0 & 0 & 0 & 0 & 0 & 0 & 0 \\ 0 & 0 & \eta_V & 0 & -(\eta_V + \eta_W + \varphi + \mu_H) & 0 & 0 & 0 & 0 & 0 & 0 \\ 0 & 0 & \eta_W & \eta_W & 0 & -\mu_H & 0 & 0 & 0 & 0 & 0 \\ 0 & 0 & \eta_W & \eta_W & 0 & -\mu_H & 0 & 0 & 0 & 0 & 0 \\ 0 & 0 & 0 & \varphi & 0 & 0 & -\mu_H & 0 & 0 & 0 & 0 \\ 0 & -\frac{\rho_A N_A}{N_H} & 0 & -\frac{\rho_A N_A}{N_H} & 0 & 0 & 0 & -\mu_A & 0 & 0 \\ 0 & \frac{\rho_A N_A}{N_H} & 0 & \frac{\rho_A N_A}{N_H} & 0 & 0 & 0 & 0 & -\mu_A & 0 \\ 0 & 0 & \theta & \theta & 0 & 0 & 0 & 0 & 0 & -\delta \end{bmatrix}$$

Using the cofactor expansion, the determinant of J becomes

$$\det |J - \lambda I| = (-(\eta_V + \eta_W + \varphi + \mu_H) - \lambda)(-\mu_H - \lambda)^4 (-\mu_A - \lambda)$$

$$[(-\theta \beta_W N_H)(\lambda^2 + (\mu_A + \eta_V + \mu_H)\lambda + (\eta_V + \mu_H)\mu_A) + (\lambda^2 + (\eta_W + \mu_H + \delta)\lambda + (\eta_W + \mu_H))(\lambda^2 + (\mu_A + \eta_V + \mu_H)\lambda + (\eta_V + \mu_H)\mu_A - \frac{\beta_V \rho_A N_A}{N_H})].$$

Hence, the eigenvalues are

$$\begin{split} &\lambda_{1} = -\eta_{V} - \eta_{W} - \mu_{H} - \varphi \\ &\lambda_{2} = -\mu_{H} (\text{multiplicity of 4}) \\ &\lambda_{3} = -\mu_{A} \\ &\lambda_{4,5} = -\frac{\eta_{V}}{2} - \frac{\mu_{A}}{2} - \frac{\mu_{H}}{2} \pm \frac{\sqrt{N_{H} (4N_{A}\beta_{V}\rho_{A} + N_{H} (\eta_{V} - \mu_{A} + \mu_{H})^{2}))}}{2N_{H}} \\ &\lambda_{6,7} = -\frac{\delta}{2} - \frac{\eta_{W}}{2} - \frac{\mu_{H}}{2} \pm \frac{\sqrt{4N_{H}\beta_{W}\theta + (\delta - \eta_{W} - \mu_{H})^{2}}}{2}. \end{split}$$

Since $\lambda_1, \lambda_2, \lambda_3$ are always negative, then the stability of DFE is determined by $\lambda_{4,5}$ and $\lambda_{6,7}$. With $\mathcal{R}_1 = \sqrt{\frac{\rho_A \beta_V N_A}{\mu_A (\eta_V + \mu_H) N_H}}$ gives

$$4N_A\beta_V\rho_A = 4N_H\mathcal{R}_1^2\mu_A(\eta_V + \mu_H)$$

and substituting it to $\lambda_{4,5}$, yields

$$\begin{split} \lambda_{4,5} &= -\frac{\eta_{V}}{2} - \frac{\mu_{A}}{2} - \frac{\mu_{H}}{2} \pm \frac{\sqrt{N_{H} \left(4N_{H} \mathcal{R}_{1}^{2} \mu_{A} (\eta_{V} + \mu_{H}) + N_{H} \left(\eta_{V} - \mu_{A} + \mu_{H}\right)^{2}\right)\right)}}{2N_{H}} \\ &= -\frac{\eta_{V}}{2} - \frac{\mu_{A}}{2} - \frac{\mu_{H}}{2} \pm \frac{\sqrt{N_{H}^{2} \left(4\mathcal{R}_{1}^{2} \mu_{A} (\eta_{V} + \mu_{H}) + \left(\eta_{V} - \mu_{A} + \mu_{H}\right)^{2}\right)\right)}}{2N_{H}} \\ \lambda_{4,5} &= -\frac{\eta_{V}}{2} - \frac{\mu_{A}}{2} - \frac{\mu_{H}}{2} \pm \frac{\sqrt{4\mathcal{R}_{1}^{2} \mu_{A} (\eta_{V} + \mu_{H}) + \left(\eta_{V} - \mu_{A} + \mu_{H}\right)^{2}}}{2}. \end{split}$$

Moreover, with $\mathcal{R}_2 = \sqrt{\frac{\theta \beta_W N_H}{\delta(\eta_W + \mu_H)}}$, gives $4N_H \beta_W \theta = 4\mathcal{R}_2^2 \delta(\eta_W + \mu_H)$. Substituting it to $\lambda_{6,7}$, the expression becomes

$$\lambda_{6,7} = -\frac{\delta}{2} - \frac{\eta_W}{2} - \frac{\mu_H}{2} \pm \frac{\sqrt{4R_2^2\delta(\eta_W + \mu_H) + (\delta - \eta_W - \mu_H)^2}}{2}.$$

Observe that $0 < \eta_V, \eta_W, \mu_H, \mu_A, \delta < 1$. Consequently, when $\mathcal{R}_1 < 1$, the term

$$\sqrt{4\mathcal{R}_1^2\mu_A(\eta_V + \mu_H) + (\eta_V - \mu_A + \mu_H)^2}$$

is real, positive, and relatively small compared to the negative terms. Similarly, when $\mathcal{R}_2 < 1$, the expression

$$\sqrt{4\mathcal{R}_2^2\delta(\eta_W + \mu_H) + (\delta - \eta_W - \mu_H)^2}$$

will not dominate the negative terms. Hence, $\lambda_{4,5,6,7}$ are all negative. Therefore, by Theorem 3.7, if $\mathcal{R}_0 = \max\{\mathcal{R}_1, \mathcal{R}_2\} < 1$, the disease-free equilibrium point $(N_H, 0, 0, 0, 0, 0, 0, 0, N_A, 0, 0)$ is locally asymptotically stable; and if $\mathcal{R}_0 > 1$, the DFE is unstable.

3.4 Sensitivity Analysis

Sensitivity analysis is performed to identify the most influential parameters for the spreading out as well as control of infection in the community. The normalized forward sensitivity index of \mathcal{R}_0 with respect to a parameter ,say p is given by

$$\gamma_p^{\mathcal{R}_0} = \frac{\partial \mathcal{R}_0}{\partial p} \times \frac{p}{\mathcal{R}_0}.$$

Positive (negative) values indicate a positive (negative) correlation with \mathcal{R}_0 , whereas the magnitude determines the importance of the parameter [8]. Since $\mathcal{R}_0 = \max\{\mathcal{R}_1, \mathcal{R}_2\}$, we obtain the sensitivity analysis of \mathcal{R}_1 and \mathcal{R}_2 separately in the following way:

$$\gamma_{\beta_V}^{\mathcal{R}_1} = \frac{\partial \mathcal{R}_1}{\partial \beta_V} \times \frac{\beta_V}{\mathcal{R}_1} \\
= \frac{1}{2} \left(\frac{\rho_A \beta_V N_A}{\mu_A (\eta_V + \mu_H) N_H} \right)^{-\frac{1}{2}} \left(\frac{\rho_A N_A}{\mu_A (\eta_V + \mu_H) N_H} \right) \left(\frac{\beta_V}{\mathcal{R}_1} \right) = \frac{1}{2}$$

$$\gamma_{\rho_A}^{\mathcal{R}_1} = \frac{\partial \mathcal{R}_1}{\partial \rho_A} \times \frac{\rho_A}{\mathcal{R}_1} \\
= \frac{1}{2} \left(\frac{\rho_A \beta_V N_A}{\mu_A (\eta_V + \mu_H) N_H} \right)^{-\frac{1}{2}} \left(\frac{\beta_V N_A}{\mu_A (\eta_V + \mu_H) N_H} \right) \left(\frac{\rho_A}{\mathcal{R}_1} \right) = \frac{1}{2}$$



$$\begin{split} & \gamma_{\eta_{V}}^{\mathcal{R}_{1}} = \frac{\partial \mathcal{R}_{1}}{\partial \eta_{V}} \times \frac{\eta_{V}}{R_{1}} \\ & = \frac{1}{2} \left(\frac{\rho_{A}\beta_{V}N_{A}}{\mu_{A}(\eta_{V} + \mu_{H})N_{H}} \right)^{-\frac{1}{2}} \left(-\frac{\rho_{A}\beta_{V}N_{A}}{\mu_{A}N_{H}(\eta_{V} + \mu_{H})^{2}} \right) \left(\frac{\eta_{V}}{\mathcal{R}_{1}} \right) = -\frac{\eta_{V}}{2(\eta_{V} + \mu_{H})} < 0 \\ & \gamma_{\mu_{A}}^{\mathcal{R}_{1}} = \frac{\partial \mathcal{R}_{1}}{\partial \mu_{A}} \times \frac{\mu_{A}}{\mathcal{R}_{1}} \\ & = \frac{1}{2} \left(\frac{\rho_{A}\beta_{V}N_{A}}{\mu_{A}(\eta_{V} + \mu_{H})N_{H}} \right)^{-\frac{1}{2}} \left(-\frac{\rho_{A}\beta_{V}N_{A}}{\mu_{A}(\eta_{V} + \mu_{H})N_{H}} \right) \left(\frac{\mu_{A}}{\mathcal{R}_{1}} \right) = -\frac{1}{2} \\ & \gamma_{\mu_{H}}^{\mathcal{R}_{2}} = \frac{\partial \mathcal{R}_{1}}{\partial \mu_{H}} \times \frac{\mu_{H}}{\mathcal{R}_{1}} \\ & = \frac{1}{2} \left(\frac{\rho_{A}\beta_{V}N_{A}}{\mu_{A}(\eta_{V} + \mu_{H})N_{H}} \right)^{-\frac{1}{2}} \left(-\frac{\rho_{A}\beta_{V}N_{A}}{\mu_{A}N_{H}(\eta_{V} + \mu_{H})^{2}} \right) \left(\frac{\mu_{H}}{\mathcal{R}_{1}} \right) = -\frac{\mu_{H}}{2(\eta_{V} + \mu_{H})} < 0 \\ & \gamma_{\beta_{W}}^{\mathcal{R}_{2}} = \frac{\partial \mathcal{R}_{2}}{\partial \theta_{W}} \times \frac{\beta_{W}}{\mathcal{R}_{2}} \\ & = \frac{1}{2} \left(\frac{\theta_{BW}N_{H}}{\delta(\eta_{W} + \mu_{H})} \right)^{-\frac{1}{2}} \left(\frac{\theta_{NH}}{\delta(\eta_{W} + \mu_{H})} \right) \left(\frac{\theta_{A}}{\mathcal{R}_{2}} \right) = \frac{1}{2} \\ & \gamma_{\delta}^{\mathcal{R}_{2}} = \frac{\partial \mathcal{R}_{2}}{\partial \theta} \times \frac{\delta}{\mathcal{R}_{2}} \\ & = \frac{1}{2} \left(\frac{\theta_{BW}N_{H}}{\delta(\eta_{W} + \mu_{H})} \right)^{-1/2} \left(-\frac{\theta_{BW}N_{H}}{\delta^{2}(\eta_{W} + \mu_{H})} \right) \left(\frac{\delta}{\mathcal{R}_{2}} \right) = -\frac{1}{2} \\ & \gamma_{\eta_{W}}^{\mathcal{R}_{2}} = \frac{\partial \mathcal{R}_{2}}{\partial \eta_{W}} \times \frac{\eta_{W}}{\mathcal{R}_{2}} \\ & = \frac{1}{2} \left(\frac{\theta_{BW}N_{H}}{\delta(\eta_{W} + \mu_{H})} \right)^{-\frac{1}{2}} \left(-\frac{\theta_{BW}N_{H}}{\delta(\eta_{W} + \mu_{H})^{2}} \right) \left(\frac{\eta_{W}}{\mathcal{R}_{2}} \right) = -\frac{\eta_{W}}{2(\eta_{W} + \mu_{H})} \\ & \gamma_{\mu_{H}}^{\mathcal{R}_{2}} = \frac{\partial \mathcal{R}_{2}}{\partial \mu_{H}} \times \frac{\mu_{H}}{\mathcal{R}_{2}} \\ & = \frac{1}{2} \left(\frac{\theta_{BW}N_{H}}{\delta(\eta_{W} + \mu_{H})} \right)^{-\frac{1}{2}} \left(-\frac{\theta_{BW}N_{H}}{\delta(\eta_{W} + \mu_{H})^{2}} \right) \left(\frac{\mu_{H}}{\mathcal{R}_{2}} \right) = -\frac{\mu_{H}}{2(\eta_{W} + \mu_{H})}. \end{split}$$

Parameters with positive sensitivity indices, such as β_V , ρ_A , β_W , and θ , play a crucial role in increasing the spread of vector-borne, waterborne diseases, and their coinfection within the community. Conversely, parameters with negative sensitivity indices, including η_V , η_W , μ_A , μ_H , and δ , are key to reducing the transmission of these diseases, highlighting their potential for disease control when their values are increased.

Parameter	Baseline Value	Sensitivity Index
eta_V	0.75	$+\frac{1}{2}$
$ ho_A$	0.375	$+\frac{1}{2}$
η_V	0.3	$-0.4\overline{286}$
μ_A	0.1	$-\frac{1}{2}$
eta_W	0.005	$+rac{1}{2}$
heta	0.0002	$+rac{1}{2}$
δ	0.5	$-rac{ar{1}}{2}$
η_W	0.2	-0.4

Table 1: Sensitivity indices of \mathcal{R}_0 evaluated at the baseline parameter values.

4 Numerical Simulation

In this section, model simulations were performed using Python to evaluate the model's behavior under different scenarios. The system of differential equations (1)–(10) was numerically solved using the adaptive Runge-Kutta method of order 45 (RK45). A semi-logarithmic scale was employed in plotting the compartmental dynamics to better illustrate exponential decay and oscillatory behavior, which are less visible in linear plots. In semi-log plots, exponential growth or decay appears as a straight line, making it easier to observe both the early fast changes and long-term behavior of the system.

The simulations were performed to evaluate model behavior under different parameter regimes and to check the stability properties of the disease-free equilibrium and endemic equilibrium. The parameter values used for the simulations are summarized in Table 3, and the initial conditions are given in Table 2.

State Variable	Description	Value
$S_H(0)$	Initial condition for susceptible humans	500,000
$I_V(0)$	Initial condition for vector-borne infected humans	7,000
$I_W(0)$	Initial condition for waterborne infected humans	4,000
$I_{VW}(0)$	Initial condition for coinfected humans	800
$R_V(0)$	Initial condition for recovered from vector-borne disease	0
$R_W(0)$	Initial condition for recovered from waterborne disease	0
$R_{VW}(0)$	Initial condition for recovered from both diseases	0
$S_A(0)$	Initial condition for susceptible vectors	200,000
$I_A(0)$	Initial condition for infected vectors	20,000
W(0)	Initial condition for waterborne pathogen concentration	100

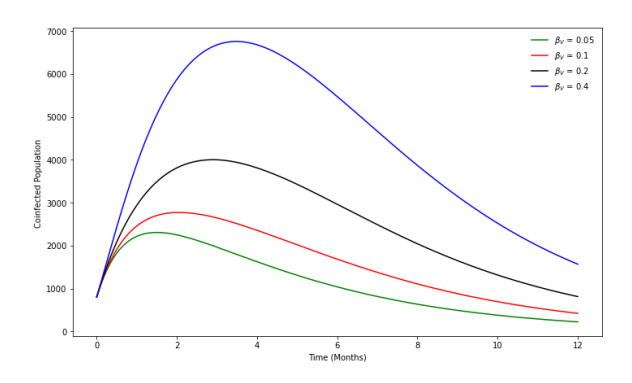
Table 2: Initial conditions of the model.



Notation	Description	Value	Source
eta_V	Transmission rate of the vector-borne disease	0.75	[5]
β_W	Transmission rate of the waterborne disease	0.005	Assumed
θ	Shedding rate of pathogens into water	0.0002	[7]
δ	Natural decay rate of the pathogen in water	0.5	[16]
η_V	Recovery rate from the vector-borne disease	0.3	[9]
η_W	Recovery rate from the water- borne disease	0.2	[10]
φ	Recovery rate from coinfection	0.05	Assumed
μ_H	Birth (and death) rate of humans	0.05	Assumed
μ_A	Birth (and death) rate of vectors	0.1	[14]
$ ho_A$	Effective contact rate for vector-borne transmission	0.375	[5, 14]

Table 3: Parameters of the model.

4.1 Effect of transmission rates β_V and β_W on coinfectious individual



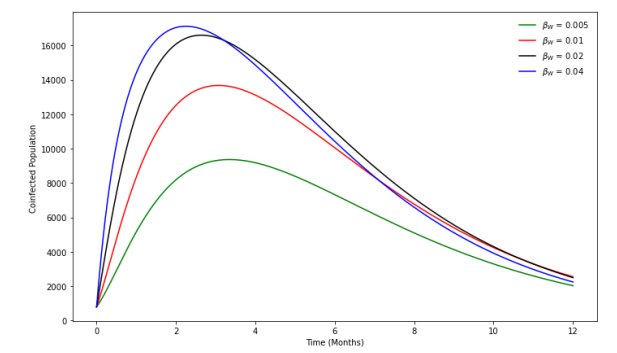


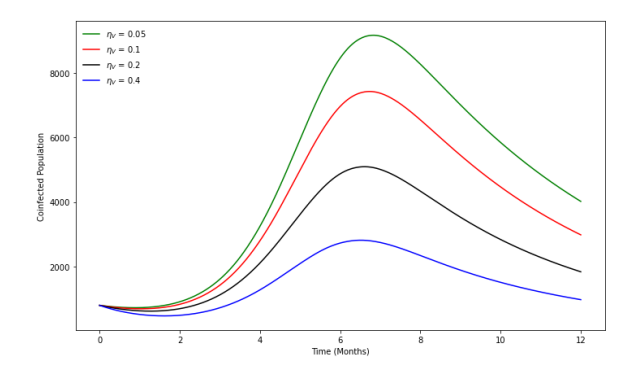
Figure 2: Effect of vector-borne transmission rate (β_V) on coinfectious population

Figure 3: Effect of waterborne transmission rate (β_W) on coinfectious population

An increase in the vector-borne transmission rate (β_V) leads to a higher number of coinfected individuals, as observed in Figure 2. This behavior is expected since a higher β_V implies an increased probability of susceptible individuals acquiring the infection through contact with infected vectors. The curve exhibits positive sensitivity, indicating that β_V significantly contributes to the spread of coinfection. Similarly, Figure 3 illustrates the effect of the waterborne transmission rate (β_W) on coinfectious individuals. Increasing β_W results in a rise in coinfection

cases due to greater exposure to contaminated water sources, demonstrating the critical role of waterborne transmission in disease persistence.

4.2 Effect of recovery rates η_V and η_W on coinfectious individual



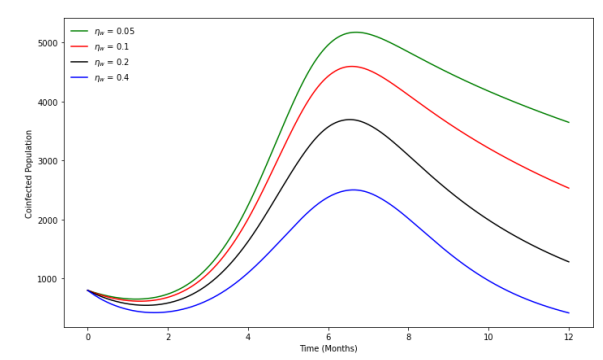


Figure 4: Effect of vector-borne recovery $rate(\eta_v)$ on coinfectious population

Figure 5: Effect of waterborne recovery $rate(\eta_w)$ on coinfectious population

On the other hand, recovery rates show an inverse relationship with the coinfected population. Figure 4 presents the effect of the vector-borne recovery rate (η_V) , where an increase in η_V reduces the number of coinfected individuals. This occurs because a higher recovery rate means infected individuals clear the infection more rapidly, reducing the duration of disease transmission. Similarly, Figure 5 displays the impact of the waterborne recovery rate (η_W) , showing that an increase in η_W leads to a decline in coinfection cases. These results highlight the importance of improving treatment strategies to accelerate recovery and mitigate disease spread.

The sensitivity analysis, as summarized in Table 1, confirms these findings. The transmission rates (β_V, β_W) have positive sensitivity indices, meaning that increasing these rates amplifies disease transmission. In contrast, the recovery rates (η_V, η_W) have negative sensitivity indices, signifying their role in reducing the infection burden. These numerical results emphasize that controlling transmission through vector and water sanitation interventions, along with enhancing recovery rates through medical treatment, are crucial strategies for mitigating the impact of coinfections.

4.3 Model Dynamics when $\mathcal{R}_0 < 1$

In Figure 6, both the vector-borne and waterborne basic reproduction numbers, \mathcal{R}_1 and \mathcal{R}_2 , are less than one. This means the infection cannot spread widely, and all the infected compartments eventually go to zero. The susceptible human population starts to decrease but later rises again, while recovered individuals increase and then stabilize. The number of infected vectors and the amount of pathogen in water also drop to zero. This shows that the system tends toward the disease-free equilibrium over time.



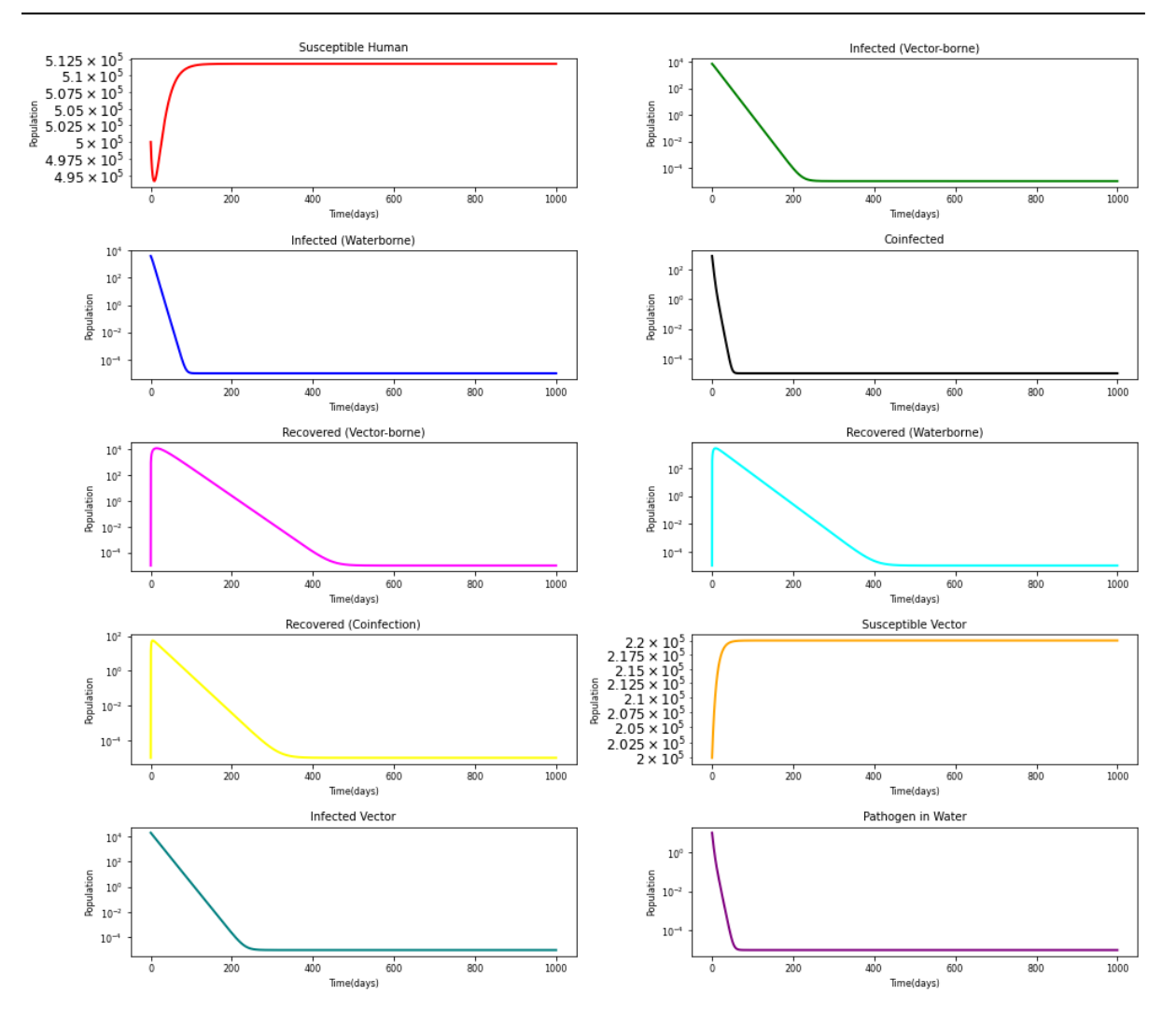


Figure 6: Plot showing the dynamics of the model compartments when $\mathcal{R}_1 \approx 0.2478 < 1$ and $\mathcal{R}_2 \approx 0.2023 < 1$. Parameter values used: $\rho_A = 0.05$, $\beta_V = 0.1$, $\theta = 0.0001$, $\beta_W = 0.0001$. These ensure $\mathcal{R}_0 < 1$.

4.4 Model Dynamics when $\mathcal{R}_0 > 1$

Figure 7 shows the behavior of all model compartments under the condition $\mathcal{R}_0 > 1$. In this scenario, the infection persists in the population. The infected human compartments, infected vectors, and environmental pathogen concentration exhibit oscillations before reaching an endemic equilibrium. The susceptible human population declines and does not return to its original level, indicating sustained transmission and the failure of the disease-free state to remain stable.

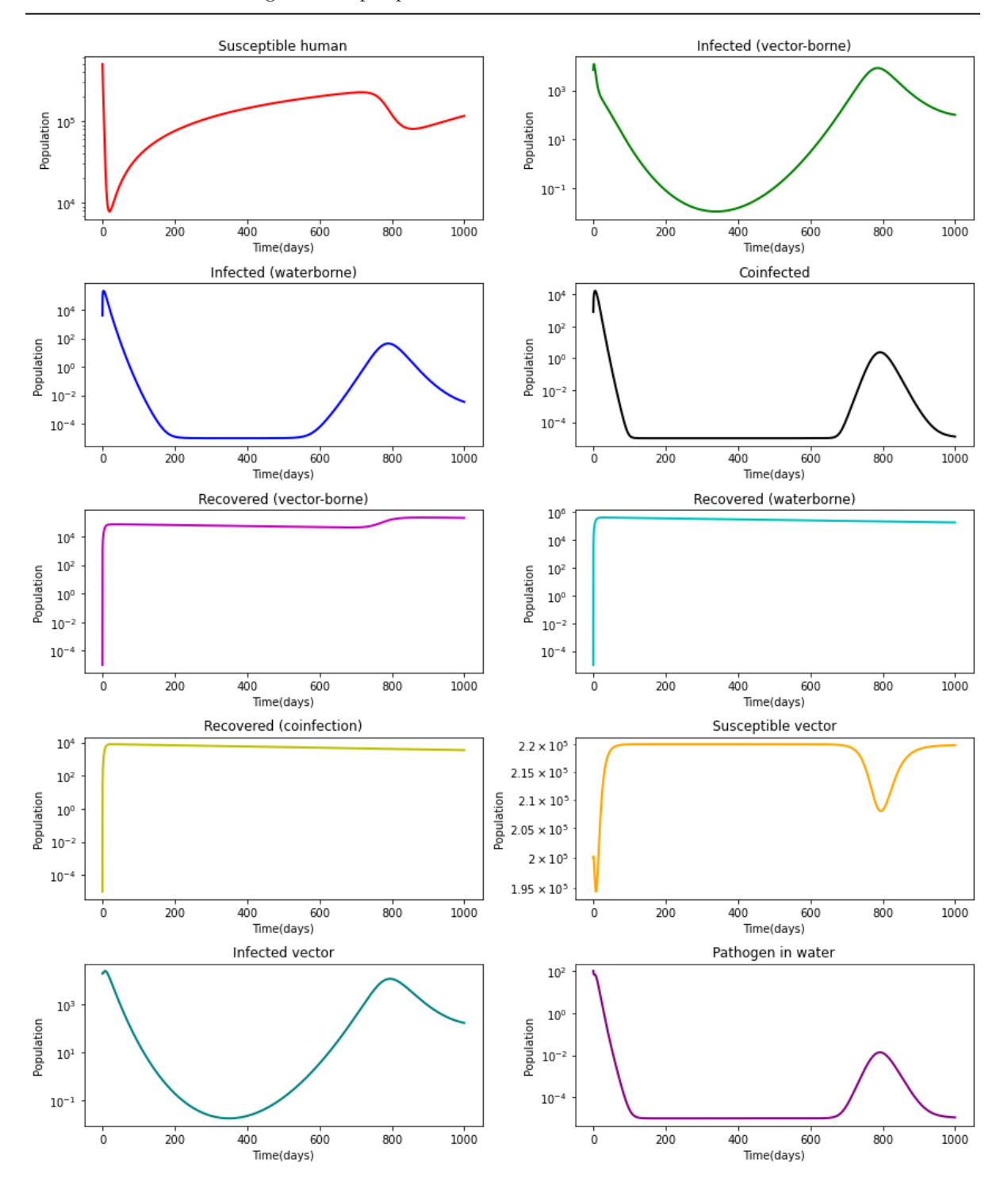


Figure 7: Plot showing the dynamics of the model compartments when $\mathcal{R}_1 > 1$ and $\mathcal{R}_2 > 1$. Parameter values used are given in Table 3. These parameter values lead to $\mathcal{R}_0 > 1$ indicating the potential for epidemic spread.

To further illustrate this behavior, Figure 8 provides a detailed view of the infected compartments. Specifically, the vector-borne infected population I_V experiences an early, sharp outbreak, followed by a secondary peak around day 770. This is primarily driven by the high transmission rate ($\beta_V = 0.75$) and the initially large infected vector population. In contrast, the waterborne infection I_W exhibits a delayed resurgence due to slower environmental accu-

mulation of pathogens governed by the shedding rate θ and decay rate δ . Figure 8 also shows that coinfection (I_{VW}) only becomes significant when both I_V and I_W rise together, around day 700. Despite starting with 800 individuals, it quickly declines and only resurges briefly, with a peak near day 800. The short duration is due to rapid recovery and removal from the coinfected class. These results highlight that the vector-borne pathway drives early transmission, while coinfection depends on the combined presence of both single infections.

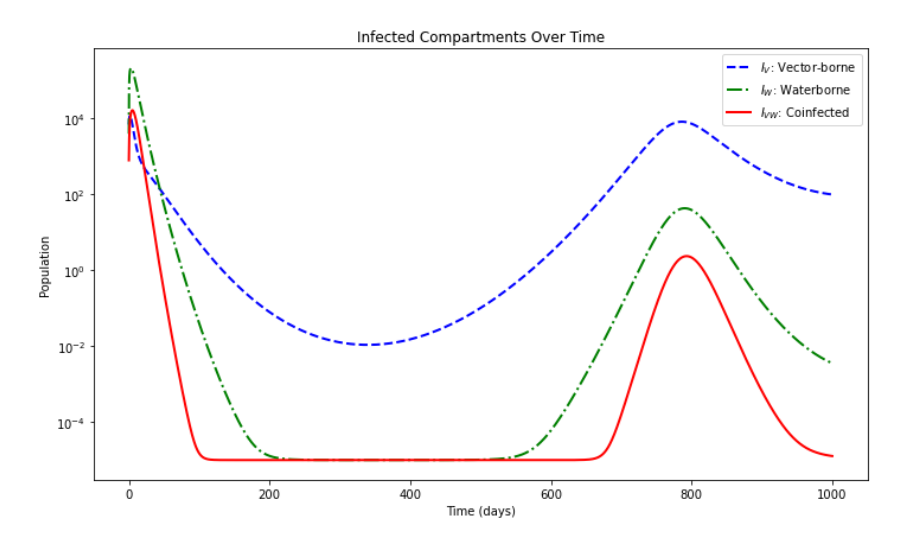


Figure 8: Dynamics over time of the vector-borne (I_V) , waterborne (I_W) , and coinfected (I_{VW}) human compartments over a 1000-day simulation.

These results show that when both reproduction numbers are less than one, the disease will eventually disappear. But if even one of them is greater than one, the infection can remain in the population for a long time. Therefore, controlling both the vector and waterborne transmission is necessary to eliminate the disease.

5 Conclusion

In this study, a mathematical model was formulated to investigate the coinfection dynamics of dengue and leptospirosis, two diseases of significant public health concern in tropical regions. The model incorporated indirect transmission mechanisms: vector-borne transmission for dengue and waterborne transmission for leptospirosis. The biological and mathematical well-posedness of the system was established by proving the positivity and boundedness of solutions within a feasible domain. Furthermore, the disease-free equilibrium was identified and analyzed using the next-generation matrix method, yielding a basic reproduction number expressed as $\mathcal{R}_0 = \max\{\mathcal{R}_1, \mathcal{R}_2\}$. The model analysis demonstrated that when both reproduction numbers are less than one, the disease-free equilibrium is locally asymptotically stable. Conversely, if either reproduction number exceeds one, the infection persists, and the system exhibits oscillatory dynamics before reaching an endemic state. Sensitivity analysis further revealed that parameters associated with transmission, such as the vector-borne transmission rate and pathogen shedding rate, positively influence disease persistence, while recovery and decay rates have mitigating effects. The numerical simulations supported the theoretical findings and provided insight into the dynamics of each compartment over time. Simulations under different scenarios illustrated the interplay between the two transmission pathways and the critical role of coinfection dynamics. It was observed that coinfection becomes significant only when both

single infections peak simultaneously. The results emphasize the need for integrated control strategies that address both vector management and water sanitation. This model provides a robust framework for understanding how dual transmission mechanisms interact and influence disease outcomes in endemic settings. For future research, it is recommended to extend the model to include seasonal variations in transmission rates, optimal control strategies such as targeted interventions, and the impact of vaccination. Further extensions may consider the incorporation of stochastic effects or spatial heterogeneity to reflect real-world complexity.

Acknowledgements

The authors are grateful to the anonymous referees for their helpful comments and the institutions for their support in the completion of this research.

References

- [1] H. Alemneh, A co-infection model of dengue and leptospirosis diseases, Adv. Differ. Equ. (2020). doi:10.1186/s13662-020-03126-6.
- [2] M. Braun, Differential Equations and Their Applications: An Introduction to Applied Mathematics, 2nd ed., Springer-Verlag, New York, 1975.
- [3] C. Caminade, K. M. McIntyre, and A. E. Jones, Impact of recent and future climate change on vector-borne diseases, Ann. N.Y. Acad. Sci. 1436 (2019), no. 1, 157–173. doi:10.1111/nyas.13950.
- [4] Cleveland Clinic, Leptospirosis. Available at: https://my.clevelandclinic.org/health/diseases/24021-leptospirosis. Accessed January 31, 2025.
- [5] M. Derouich, A. Boutayeb, and E. H. Twizell, *A model of Dengue fever*, Biomed. Eng. Online **2** (2003), 4. doi:10.1186/1475-925X-2-4.
- [6] O. Diekmann, J. A. P. Heesterbeek, and J. A. J. Metz, On the definition and computation of the basic reproduction ratio R₀ in models for infectious diseases in heterogeneous populations, J. Math. Biol. 28 (1990), 365–382. doi:10.1007/BF00178324.
- [7] H. A. Engida, D. M. Theuri, D. Gathungu, J. Gachohi, and H. T. Alemneh, A mathematical model analysis for the transmission dynamics of leptospirosis disease in human and rodent populations, Comput. Math. Methods Med. (2022), Article ID 1806585. doi:10.1155/ 2022/1806585.
- [8] F. N. Ngoteya and Y. Nkansah-Gyekye, Sensitivity analysis of parameters in a competition model, Appl. Comput. Math. 4 (2015), no. 5, 363–368. doi:10.11648/j.acm.20150405.15.
- [9] S. M. Garba, A. B. Gumel, and M. A. Bakar, *Backward bifurcations in dengue transmission dynamics*, Math. Biosci. **215** (2008), no. 1, 11–25. doi:10.1016/j.mbs.2008.05.002.
- [10] M. A. Khan, S. F. Saddiq, S. Islam, I. Khan, and S. Shafie, Dynamic behavior of leptospirosis disease with saturated incidence rate, Int. J. Appl. Comput. Math. 2 (2016), 435–452. doi:10.1007/s40819-015-0102-2.
- [11] A. Ko, C. Goarant, and M. Picardeau, Leptospira: the dawn of the molecular genetics era for an emerging zoonotic pathogen, Nat. Rev. Microbiol. 7 (2009), 736–747. doi:10.1038/nrmicro2208.



- [12] R. Larson, Elementary Linear Algebra, 8th ed., Cengage Learning, 2016.
- [13] H. Leclerc, L. Schwartzbrod, and E. Dei-Cas, Microbial agents associated with waterborne diseases, Crit. Rev. Microbiol. 28 (2002), 371–409. doi:10.1080/1040-840291046768.
- [14] D. P. Lizarralde-Bejarano, S. Arboleda-Sánchez, and M. E. Puerta-Yepes, *Understanding epidemics from mathematical models: Details of the 2010 dengue epidemic in Bello (Antioquia, Colombia)*, Appl. Math. Model. **43** (2017), 566–578. doi:10.1016/j.apm.2016.11.022.
- [15] G. Macdonald, The Epidemiology and Control of Malaria, Oxford University Press, 1957.
- [16] A. Minter, F. Costa, H. Khalil, J. Childs, P. Diggle, A. I. Ko, and M. Begon, *Optimal control of rat-borne leptospirosis in an urban environment*, Front. Ecol. Evol. **7** (2019), 209. doi:10.3389/fevo.2019.00209.
- [17] R. Nagraik, A. Kaushal, S. Gupta, A. Sharma, and D. Kumar, Leptospirosis: A systematic review, J. Microbiol. Biotechnol. Food Sci. 9 (2020), no. 6, 1099–1109. doi:10.15414/ jmbfs.2020.9.6.1099–1109.
- [18] O. F. Nwabor, E. I. Nnamonu, P. E. Martins, and O. C. Ani, Water and waterborne diseases: A review, Int. J. Trop. Dis. Health 12 (2016), no. 4, 1–14. doi:10.9734/IJTDH/ 2016/21895.
- [19] R. Ross, The Prevention of Malaria, John Murray, London, 1911.
- [20] J. H. Tien and D. J. Earn, Multiple transmission pathways and disease dynamics in a waterborne pathogen model, Bull. Math. Biol. **72** (2010), no. 6, 1506–1533. doi:10.1007/s11538-010-9507-6.
- [21] S. Tiwari et al., Prevalence of dengue and leptospirosis coinfection and associated mortality rates: A systematic review and meta-analysis, BMC Infect. Dis. 25 (2025), 111. doi: 10.1186/s12879-025-10498-1.
- [22] P. van den Driessche and J. Watmough, Reproduction numbers and sub-threshold endemic equilibria for compartmental models of disease transmission, Math. Biosci. 180 (2002), 29–48. doi:10.1016/S0025-5564(02)00108-6.
- [23] P. van den Driessche, Reproduction numbers of infectious disease models, Infect. Dis. Model. **2** (2017), no. 3, 288–303. doi:10.1016/j.idm.2017.06.002.
- [24] World Health Organization, Fact sheet: Vector-borne diseases, 2024. Available at: https://www.who.int/news-room/fact-sheets/detail/vector-borne-diseases.